

Layer buckling and absence of superconductivity in LaNiO₂

S. Rathnayaka,¹ S. Yano,^{1,2} K. Kawashima,³ J. Akimitsu,³ C.M. Brown,^{4,5} J. Neufeind,⁶ and D. Louca^{1,*}

¹*University of Virginia, Department of Physics, Charlottesville, Virginia 22904, U.S.A.*

²*Neutron Group, National Synchrotron Radiation Research Center, Hsinchu, 30076 Taiwan, Republic of China*

³*Department of Physics and Mathematics, Aoyama Gakuin University,
5-10-1 Fuchinobe, Sagamihara, KANAGAWA 252-5258, Japan*

⁴*NIST Center for Neutron Research, National Institute of Standards and Technology,
100 Bureau Drive, MS 6100, Gaithersburg, MD 20899-6100, U.S.A.*

⁵*Department of Chemical Engineering, University of Delaware, Newark, DE 19716, U.S.A.*

⁶*Spallation Neutron Source, Oak Ridge National Laboratory, Oak Ridge, TN 37831, U.S.A.*

The recent observation of unconventional superconductivity in thin films of LaNiO₂ (critical temperature, $T_c \sim 10$ K) and in bulk single crystals of La₃Ni₂O₇ (327) under pressure ($T_c \sim 80$ K), has brought to light a long sought-after class of superconducting nickelates. Through structural measurements in the 327-system, it was shown that the absence of superconductivity is related to bending of the O-Ni-O bonds. Similarly, the bond bending may be linked to the absence of superconductivity in bulk LaNiO₂. Neutron diffraction was used on bulk non-superconducting La_{1-x}Sr_xNiO₂ samples to show that the layers are naturally buckled, creating a Ni-O-Ni bond angle of 177° at 2 K and ambient pressure. The buckling angle increases to 170° on warming to room temperature. Furthermore, a broad paramagnetic continuum is observed that decreases in intensity on cooling from room temperature signaling a possible transition to a coherent state. However, no antiferromagnetic (AFM) peaks are detected, although enhancement of ferromagnetic (FM) correlations cannot be excluded.

High temperature superconductivity in cuprates whose parent compound is an AFM insulator has driven much of the research in strongly correlated electron systems[1]. In this class, the CuO₂ plane is a critical component of superconductivity, intimately related to the band position and hybridization between the $d_{x^2-y^2}$ and $d_{z^2-r^2}$ orbitals that influence the shape of the Fermi surface and the transition temperature. The distance of the Cu ion from the apical oxygen is significant to the hybridization and the transition temperature as predicted by the Maekawa plot[2]. Recently, superconductivity was reported in (La,Sr)NiO₂ films and in Nd doped Nd_{1-x}Sr_xNiO₂ with a $T_c \sim 10$ K[3, 4]. RENiO₂ (RE – rare earth) with an infinite layered structure (Fig. 1(a)), is isostructural to (Ca,Sr)CuO₂, the parent compound of Sr_{1-x}Nd_xCuO₂ ($T_c \sim 34$ K) and Sr_{1-x}La_xCuO₂ ($T_c \sim 43$ K). Electronic band structure calculations indicated that the bands near E_F in LaNiO₂ resemble that of CaCuO₂[5]. The Ni¹⁺ ion in the 3d⁹ electronic configuration is similar to the electronic state of the Cu²⁺ ion with $S = 1/2$ (see inset of Fig. 1(b) for a simple representation of the orbital states)[6–10]. Little is known of the contribution of magnetism to the superconducting mechanism while observations of superconductivity in lanthanum doped systems rules out the influence of the RE moment. Resonant inelastic X-ray scattering on NdNiO₃ indicated dispersive excitations with about 200 meV width, reminiscent of spin waves arising from an AFM lattice[11].

LaNiO₂ is synthesized by reducing the perovskite LaNiO₃ to the infinite layered structure[12–14]. The electronic configuration of Ni¹⁺ (3d⁹) in the square pla-

nar configuration is shown in the inset of Fig. 1(b). According to the Goodenough-Kanamori rules, the interaction of the Ni-O-Ni via 180° degrees ought to be AFM [15, 16] if the spin is localized. A previous neutron diffraction study indicated no long-range magnetic order down to 5 K[13]. Whether or not a magnetic ground state is present in LaNiO₂ is revisited using both reactor-based and spallation neutron sources. Moreover, the local atomic structure is probed in search for evidence of layer buckling and its implications on Ni-O-Ni coupling. It was previously reported that LaNiO₂ is a Mott insulator in the ground state, and remains paramagnetic down to 5 K[13, 14]. Our magnetic susceptibility data both for pure and Sr doped LaNiO₂ plotted in Fig. 1(b) show no evidence of a magnetic transition, consistent with earlier measurements[13]. The Sr-doped samples are also paramagnetic down to low temperatures.

The polycrystalline samples of La_{1-x}Sr_xNiO₂ were synthesized using an alkali molten solution and CaH₂ oxygen reduction method as described in Ref. [12]. The sample crystallinity was confirmed using powder X-ray diffraction (XRD), where data were collected on a Multi Flex system with a graphite monochromator. The dc-magnetic susceptibility measurements were performed using a superconducting quantum interference device. The data were collected in field-cooled mode under an applied magnetic field of $H = 1$ kOe (1 Oe = (1000/4 π) A/m). Specific heat measurements were also performed on the samples in search of phase transitions.

The neutron scattering experiments were performed at the BT-1 high resolution diffractometer of the NIST Center for Neutron Research (NCNR) [17] in the temperature range of 5 to 300 K and at the Nanoscale Ordered Materials Diffractometer (NOMAD) at the Spallation Neutron

* Corresponding author; louca@virginia.edu

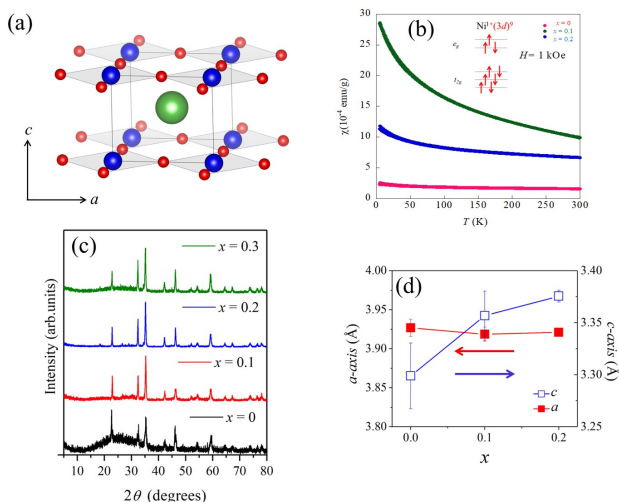


Figure 1. (a) The crystal structure of LaNiO₂ with P4/mmm symmetry. (b) The temperature dependence of the magnetic susceptibility of La_{1-x}Sr_xNiO₂ for $x = 0, 0.1$ and 0.2 under an applied magnetic field of $H = 1$ kOe ($1 \text{ Oe} = (1000/4\pi) \text{ A/m}$, $1 \text{ emu/g} = 1 \text{ Am}^2/\text{kg}$). The inset is a schematic of the electronic configuration of Ni²⁺ in NiO₂ square lattice. (c) Powder X-ray diffraction data of La_{1-x}Sr_xNiO₂ ($x = 0, 0.1, 0.2, 0.3$). (d) Lattice parameters a and c as a function of Sr²⁺ concentration x . Error bars indicate 1σ .

Source of Oak Ridge National Laboratory. Because of the difficulty of making large amount of power sample (~ 2 g), the highest neutron flux condition (monochromator: Ge (311), collimation: 60, wavelength: 2.079 Å) was used at BT-1 while at NOMAD, a white beam was used. The Rietveld refinement[18, 19] results are summarized in Table I. The NOMAD[20] data was normalized, and Fourier transformed to obtain the pair density function (PDF), $\rho(r)$. The PDF is a real-space representation of the atomic correlations. It corresponds to the probability of finding a pair of atoms separated by a distance r by averaging snapshots of pairs over time. Details of this technique can be found in Ref. [21]. The NOMAD provides high momentum transfer, Q , and data up to 40 \AA^{-1} was used for the PDF analysis. The instrumental background and empty can were subtracted from the data, followed by a normalization with vanadium. Corrected data were normalized to obtain the total structure factor, $S(Q)$. The $S(Q)$ was Fourier transformed to obtain the pair correlation function. This method has been applied successfully in many oxide systems[22, 23].

Fig. 1(c) is a plot of the X-ray diffraction data for $0 < x < 0.3$ at room temperature. The refinement yields the tetragonal symmetry, P4/mmm[13]. Pure LaNiO₂ is very close to its presumed stoichiometry, with very little oxygen, if any, at the apical site[13, 26]. Shown in Fig. 1(d) is a plot of the lattice constants as a function of doping. Note that while the a -axis barely changes with doping, the c -axis expands as expected with the Sr substitution. Neutron powder diffraction data collected at

Table I. The lattice parameters and bond length as a function of temperature. Values in parentheses indicate 1σ .

T(K)	a(Å)	a(Å)	4*Ni-O(Å)	8*La-O(Å)
300	3.9544(3)	3.4158(5)	1.9772(2)	2.6133(2)
250	3.9527(3)	3.4132(5)	1.9763(1)	2.6115(2)
200	3.9510(3)	3.4118(4)	1.9754(1)	2.6103(2)
150	3.9497(3)	3.4071(4)	1.9749(1)	2.6084(2)
100	3.9483(3)	3.4027(5)	1.9740(2)	2.6066(3)
70	3.9480(3)	3.4040(4)	1.9740(1)	2.6068(2)
50	3.9477(3)	3.4023(4)	1.9739(1)	2.6060(2)
30	3.9476(3)	3.4029(3)	1.9738(1)	2.6061(2)
5	3.9479(3)	3.4032(4)	1.9738(1)	2.6064(2)

Table II. The calculated momentum transfer, Q , positions and magnetic form factor for potential magnetic Bragg peaks.

(hkl)	$Q(\text{\AA}^{-1})$	$f_{\text{mag}}(Q)^2$	Reference
(0.5 0 0)	0.7959	0.9204	
(0 0 0.5)	0.9224	0.9077	
(0.5 0 0.5)	1.2183	0.8266	SrCuO ₂ [15]
(0.5 0.5 0.5)	1.4553	0.7647	Ca _{0.85} Sr _{0.15} CuO ₂ [24], SeFeO ₂ [25]

the BT-1 powder diffractometer of the NIST Center for Neutron Research (NCNR) on pure LaNiO₂ at 5 and 300 K are shown in Fig. 2. The data at 5 K, collected over a 24-hour period, is compared to the 300 K data, the latter multiplied by a factor of 10 as shown in the intensity versus momentum transfer (Q) plot. The anticipated AFM magnetic peak positions in reciprocal space based on several possible AFM propagation vectors are listed in Table II[24, 25, 27], considering the magnetic form factor of Ni²⁺ [28]. No new Bragg peaks are observed at 5 K that are not otherwise present at 300 K, indicating that no static long-range magnetic order in LaNiO₂ down to 5 K. Magnetic fluctuations may persist however, and this will be discussed below.

The analysis of the neutron diffraction data also yields the oxygen thermal factors shown in Fig. 2(b). The thermal factor along the z -direction is larger than the ones corresponding to thermal motion in the ab -plane, which may serve as indication of distortions along this direction. The lattice parameters, a and c , linearly increase with increasing temperature in pure LaNiO₂ as shown in Fig. 2(c) where a negative thermal expansion behavior is observed in the c -lattice constant below 50 K. Also shown in Fig. 2(d) is the specific heat that smoothly increases with increasing temperature. With the substitution of Sr²⁺ as in La_{1-x}Sr_xNiO₂ ($x = 0.1, 0.2, 0.3$), no structural phase transition is observed. The observed diffraction peaks can also be indexed by a tetragonal unit cell (Fig. 1(c)). As seen in Fig. 1(d), the c -lattice parameter increases with the Sr substitution, which is indication that Sr enters the lattice. Attempts to synthesize samples with higher Sr²⁺ concentration were unsuccessful.

Shown in Fig. 3 is a plot of the structure function,

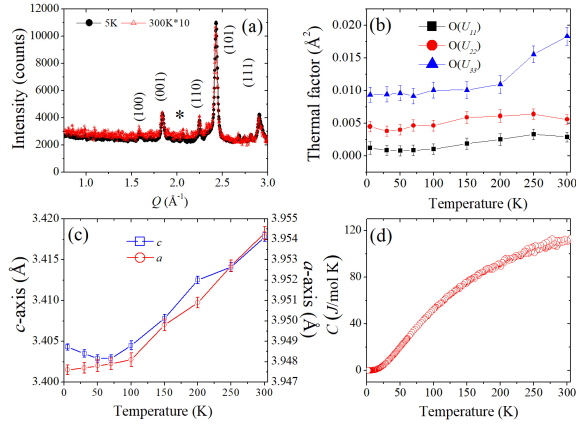


Figure 2. (a) Powder neutron diffraction patterns of LaNiO_2 at 5 K and 300 K from BT-1 (the 300 K data were multiplied by 10). The peaks indexed as * are observed both at 5 K and 300 K. These peaks are close to (0.5 0.5 1) but not exactly. The calculated and observed Q are 2.068 \AA^{-1} and 2.155 \AA^{-1} at 300 K, 2.070 \AA^{-1} and 2.162 \AA^{-1} at 5 K. (b) The oxygen thermal factors in LaNiO_2 obtained by the Rietveld refinement method are plotted as a function of temperature. (c) The temperature dependence of the lattice constants a and c for LaNiO_2 . (d) The specific heat of LaNiO_2 as a function of temperature shows no evidence of a transition. Error bars indicate 1σ .

$S(Q)$, obtained from NOMAD, on powder LaNiO_2 as a function of temperature. Even though the instrument background and empty can were subtracted from the data, the $S(Q)$ exhibits a broad continuum that is temperature dependent. The data shown in the figure are not shifted and the reduction in the background occurs on cooling. The difference in the $S(Q)$ between temperatures is shown in the difference plot below (over a larger Q -range). The changes are more pronounced at low Q . The origin of the broad continuum can be twofold: either it signals the presence of magnetic diffuse scattering or it arises from lattice disorder. In the first scenario, it is reasonable to expect that if the paramagnetic fluctuations are reduced upon cooling, this may lead to an ordered state. No AFM peaks have been detected however i.e. no extra Bragg peaks are evident in the data from both sets of measurements (BT-1 and NOMAD). On the other hand, the condensation of fluctuating spins may produce FM interactions. Given the absence of a magnetic transition in the bulk susceptibility, there is no long-range FM transition, but FM correlations are still possible. Careful examination of the nuclear Bragg peaks at low momentum transfers indicates subtle changes, but it is difficult to discern that any change in the nuclear Bragg intensity is solely due to ferromagnetism. With regards to scenario two, defects or other lattice effects may contribute to the elevated background. While the presence of interstitials and vacancies were ruled out from the refinement of the diffraction data, distortions of the square lattice

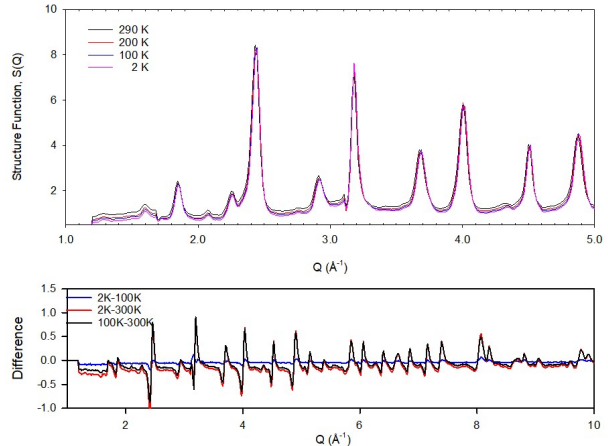


Figure 3. (a) The structure function, $S(Q)$, obtained from the NOMAD neutron diffraction data is plotted at several temperatures. The instrumental background, empty can and normalization with vanadium was performed at all temperatures. The broad diffuse background observed at low Q decreases with cooling. This can be seen in (b) that plots the difference between (2-100)K, (2-300)K and (100-300)K.

are possible and discussed next.

The Fourier transform of the structure function shown in Fig. 3 yields the correlation function, $G(r)$. The $G(r)$ corresponding to the local atomic structure of LaNiO_2 at 2 K is shown in Fig. 4(a). The peaks correspond to the probability of finding a particular atom pair in real-space. The first peak corresponds to the shortest atom-atom correlation length in the crystal and that is from Ni-O pairs. Following are the La-O and O-O correlations and so on. Also shown in the plot is a calculation (solid line) based on a local tetragonal model that shown in Fig. 4(b). In this model, the oxygen atoms are displaced out of plan, in an up/down direction, and consistent with the large z -thermal factors. Specifically, in this model, the oxygen ions along the a - and b -axes are displaced up and down along the c -direction, creating a wave-like motion that buckles the infinite layer in LaNiO_2 . The displacements are antiparallel between sites and are 0.05 \AA in magnitude at 2 K. The up/down distortions of oxygen increase to $\approx 0.17 \text{ \AA}$ by room temperature. This model fits the data very well which indicates that the planes are not flat and buckling of the planes is most likely present (Fig. 4(d/e)). The distortions are analogous to what was observed previously in SrFeO_2 , an AFM insulator, with the same crystal structure (see Refs. [29]). In Fig. 4(c), the temperature dependence of the Ni-O-Ni bond angle is shown. At 2 K, the angle deviates from 180° by 3 degrees. Upon further warming, the buckling increases as shown in Figs. 4(b) and 4(d/e). This behavior was also observed in SrFeO_2 [29], but the buckling here is less. To conclude,

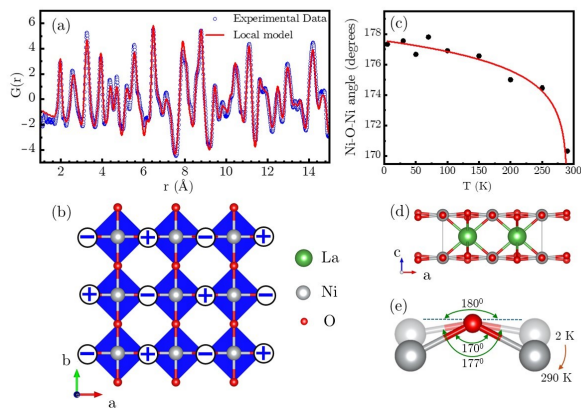


Figure 4. (a) The pair correlation function, $G(r)$, corresponding to the local atomic structure of LaNiO_2 for powder diffraction data collected at 2 K is compared to a local model shown in (b). (b) The local model consists of alternating oxygen vertical displacements along the a -direction. The + and - signs correspond to displacements in the positive or negative z -direction. The displacements are $\approx 0.05 \text{ \AA}$ at 2 K, increasing steadily to 0.17 \AA by room temperature. (c) A plot of the Ni-O-Ni bond angle as a function of temperature. Starting at 2 K, the bond is bent away from 180° , while the bending continuously increases with warming. (d) and (e) are side views of the bond bending.

the $\text{La}_{1-x}\text{Sr}_x\text{NiO}_2$ system was investigated with neutron scattering techniques. The results were complimented by bulk susceptibility and heat capacity measurements.

No long-range magnetic order is present although magnetic fluctuations may persist down to low temperatures. Moreover, the infinite layer is buckled as shown by the local structure analysis. This buckling may be contribute significantly to the absence of superconductivity. If superconductivity were to be observed, this system would benefit from a flat NiO_2 plane. We postulate that superconductivity may be observed in thin films as a result of strain induced 180° O-Ni-O bond angles that are conducive to superconductivity. Unbuckling the Ni-O bond was proven to be important to the presence of superconductivity in the 327 system [30].

This work has been supported by the Department of Energy, Grant number DE-FG02-01ER45927. We acknowledge the support of the National Institute of Standards and Technology, U. S. Department of Commerce, in providing the neutron research facilities used in this work. Work at ORNL was supported by the US Department of Energy, Office of Basic Energy Sciences, Materials Sciences and Engineering Division and Scientific User Facilities Division. Support for this work was also provided by the High-tech Research Center Project for Private Universities from the Ministry of Education, Culture, Sports, Science and Technology (MEXT), Grant-in-Aid for Specially promoted Research (JSPS KAKENHI Grant Number 25000003), and Grant-in-Aid for Scientific Research (S) and (B) (JSPS KAKENHI Grant Number 25220803 and 25287087). Moreover, this research was supported by the Strategic International Collaborative Research Program (SICORP (LEMSUPER)) from JST, Japan Science and Technology Agency. Two of authors (KK and JA) were supported by IMRA MATERIAL CO., LTD.

-
- [1] J. G. Bednorz and K. A. Müller, “Possible high T_c superconductivity in the Ba-La-Cu-O system,” *Zeitschrift für Physik B Condensed Matter* **64**, 189–193 (1986).
- [2] Y. Ohta, T. Tohyama, and S. Maekawa, “Apex oxygen and critical temperature in copper oxide superconductors: Universal correlation with the stability of local singlets,” *Physical Review B* **43**, 2968 (1991).
- [3] D. Li, K. Lee, Bai Y. Wang, M. Osada, S. Crossley, H. R. Lee, Y. Cui, Y. Hikita, and H. Y. Hwang, “Superconductivity in an infinite-layer nickelate,” *Nature* **572**, 624–627 (2019).
- [4] M. Osada, B. Y. Wang, B. H. Goodge, S. P. Harvey, K. Lee, D. Li, L. F. Kourkoutis, and H. Y. Hwang, “Nickelate superconductivity without rare-earth magnetism: (La, Sr) NiO_2 ,” *Advanced Materials* **33**, 2104083 (2021).
- [5] H. Sakakibara, H. Usui, K. Kuroki, R. Arita, and H. Aoki, “Two-orbital model explains the higher transition temperature of the single-layer Hg-cuprate superconductor compared to that of the La-cuprate superconductor,” *Physical review letters* **105**, 057003 (2010).
- [6] T. Siegrist, S.M. Zahurak, D.W. Murphy, and R.S. Roth, “The parent structure of the layered high-temperature superconductors,” *nature* **334**, 231–232 (1988).
- [7] M. Azuma, Z. Hiroi, M. Takano, Y. Bando, and Y. Takeda, “Superconductivity at 110 K in the infinite-layer compound $(\text{Sr}_{1-x}\text{Ca}_x)_{1-y}\text{CuO}_2$,” *Nature* **356**, 775–776 (1992).
- [8] M.G. Smith, A. Manthiram, J. Zhou, J.B. Goodenough, and J.T. Markert, “Electron-doped superconductivity at 40 K in the infinite-layer compound $\text{Sr}_{1-y}\text{Nd}_y\text{CuO}_2$,” *nature* **351**, 549–551 (1991).
- [9] G. Era, Y. Miyamoto, F. Kanamaru, and S. Kikkawa, “Superconductivity in the infinite-layer compound $\text{Sr}_{1-x}\text{La}_x\text{CuO}_2$ prepared under high pressure,” *Physica C: Superconductivity* **181**, 206–208 (1991).
- [10] K.W. Lee and W.E. Pickett, “Infinite-layer LaNiO_2 : Ni^{1+} is not Cu^{2+} ,” *Physical Review B* **70**, 165109 (2004).
- [11] H. Lu, M. Rossi, A. Nag, M. Osada, D.F. Li, K. Lee, B.Y. Wang, M. Garcia-Fernandez, S. Agrestini, Z.X. Shen, *et al.*, “Magnetic excitations in infinite-layer nickelates,” *Science* **373**, 213–216 (2021).
- [12] P. Crespin, M. Levitz and L. Gatineau, “*J Chem Soc Faraday*,” II **79**, 1181 (1983).

- [13] M.A. Hayward, M.A. Green, M.J. Rosseinsky, and J. Sloan, "Sodium hydride as a powerful reducing agent for topotactic oxide deintercalation: synthesis and characterization of the nickel (I) oxide LaNiO_2 ," *Journal of the American Chemical Society* **121**, 8843–8854 (1999).
- [14] T. Takamatsu, M. Kato, T. Noji, and Y. Koike, "Low-temperature synthesis of the infinite-layer compound LaNiO_2 using CaH_2 as reductant," *Physica C: Superconductivity and its applications* **470**, S764–S765 (2010).
- [15] J. B. Goodenough, "Theory of the role of covalence in the perovskite-type manganites $[\text{La}, \text{M}(\text{II})]\text{MnO}_3$," *Physical Review* **100**, 564 (1955).
- [16] J. Kanamori, "Superexchange interaction and symmetry properties of electron orbitals," *Journal of Physics and Chemistry of Solids* **10**, 87–98 (1959).
- [17] Certain commercial equipment, instruments, or materials are identified in this document. Such identification does not imply recommendation or endorsement by the National Institute of Standards and Technology, nor does it imply that the products identified are necessarily the best available for the purpose..
- [18] A.C. Larson and R.B. Von Dreele, "General structure analysis system (gsas); report LAUR 86-748," Los Alamos National Laboratory, Los Alamos, NM (2000).
- [19] B. H. Toby, "EXPGUI, a graphical user interface for GSAS," *J. Applied Cryst.* **34**, 210–213 (2001).
- [20] J. Neufelnd, M. Feygenson, J. Carruth, R. Hoffmann, and K. K. Chipley, "The nanoscale ordered materials diffractometer NOMAD at the spallation neutron source SNS," *Nuclear Instruments and Methods in Physics Research Section B: Beam Interactions with Materials and Atoms* **287**, 68–75 (2012).
- [21] B.H. Toby and T. Egami, "Accuracy of pair distribution function analysis applied to crystalline and non-crystalline materials," *Acta Crystallographica Section A: Foundations of Crystallography* **48**, 336–346 (1992).
- [22] D. Louca and T. Egami, "Local lattice distortions in $\text{La}_{1-x}\text{Sr}_x\text{MnO}_3$ studied by pulsed neutron scattering," *Physical Review B* **59**, 6193 (1999).
- [23] D. Louca, T. Egami, E. L. Brosha, H. Röder, and A.R. Bishop, "Local Jahn-Teller distortion in $\text{La}_{1-x}\text{Sr}_x\text{MnO}_3$ observed by pulsed neutron diffraction," *Physical Review B* **56**, R8475 (1997).
- [24] D. Vaknin, E. Caignol, P.K. Davies, J.E. Fischer, D.C. Johnston, and D.P. Goshorn, "Antiferromagnetism in $(\text{Ca}_{0.85}\text{Sr}_{0.15})\text{CuO}_2$, the parent of the cuprate family of superconducting compounds," *Physical Review B* **39**, 9122 (1989).
- [25] Y. Tsujimoto, C. Tassel, N. Hayashi, T. Watanabe, H. Kageyama, K. Yoshimura, M. Takano, M. Ceretti, C. Ritter, and W. Paulus, "Infinite-layer iron oxide with a square-planar coordination," *Nature* **450**, 1062–1065 (2007).
- [26] J.A. Alonso, M.J. Martínez-Lope, J.L. García-Muñoz, and M.T. Fernández-Díaz, "A structural and magnetic study of the defect perovskite from high-resolution neutron diffraction data," *Journal of Physics: Condensed Matter* **9**, 6417 (1997).
- [27] I.A. Zaliznyak, C. Broholm, M. Kibune, M. Nohara, and H. Takagi, "Anisotropic spin freezing in the $S=1/2$ zigzag chain compound SrCuO_2 ," *Physical Review Letters* **83**, 5370 (1999).
- [28] To calculate the magnetic form factor for Ni^{1+} the values are obtained from, <https://www.ill.eu/sites/ccsl/ffacts/>.
- [29] J. Li, B. and Woods, J. Siewenie, H. Hah, Jacqueline A. Johnson, C. E. Johnson, and D. Louca, "The magnetic and crystal structures of $\text{Sr}_{1-x}\text{FeO}_{2-x}\text{F}_x$, a new oxyfluoride," *Chemical Communications* **52**, 2386–2389 (2016).
- [30] H. Sun, M. Huo, X. Hu, J. Li, Z. Liu, Y. Han, L. Tang, Z. Mao, P. Yang, B. Wang, J. Cheng, D-X. Yao, Zhang G-M., and M. Wang, "Signatures of superconductivity near 80 k in a nickelate under high pressure," *Nature* **621**, 493 (2023).